Physics

Physics Research Publications

Purdue University   *Year* 2004

Constraints on the very high energy emission from BL Lacertae objects

D. Horan, H. M. Badran, I. H. Bond, P. J. Boyle, S. M. Bradbury, J. H. Buckley, D. A. Carter-Lewis, M. Catanese, O. Celik, W. Cui, M. Daniel, M. D'Vali, I. D. C. Perez, C. Duke, A. Falcone, D. J. Fegan, S. J. Fegan, J. P. Finley, L. F. Fortson, J. A. Gaidos, S. Gammell, K. Gibbs, G. H. Gillanders, J. Grube, J. Hall, T. A. Hall, D. Hanna, A. M. Hillas, J. Holder, A. Jarvis, M. Jordan, G. E. Kenny, M. Kertzman, D. Kieda, J. Kildea, J. Knapp, K. Kosack, H. Krawczynski, F. Krennrich, M. J. Lang, S. Le Bohec, E. Linton, J. L. Evans, A. Milovanovic, P. Moriarty, D. Muller, T. Nagai, S. Nolan, R. A. Ong, R. Pallassini, D. Petry, B. Power-Mooney, J. Quinn, M. Quinn, K. Ragan, P. Rebillot, P. T. Reynolds, H. J. Rose, M. Schroedter, G. H. Sembroski, S. P. Swordy, A. Syson, V. V. Vassiliev, S. P. Wakely, G. Walker, T. C. Weekes, and J. Zweerink

CONSTRAINTS ON THE VERY HIGH ENERGY EMISSION FROM BL LACERTAE OBJECTS

D. HORAN,[1] H. M. BADRAN,[2] I. H. BOND,[3] P. J. BOYLE,[4] S. M. BRADBURY,[3] J. H. BUCKLEY,[5] D. A. CARTER-LEWIS,[6] M. CATANESE,[1]
O. CELIK,[7] W. CUI,[8] M. DANIEL,[8] M. D'VALI,[3] I. DE LA CALLE PEREZ,[3] C. DUKE,[9] A. FALCONE,[8] D. J. FEGAN,[10] S. J. FEGAN,[1]
J. P. FINLEY,[8] L. F. FORTSON,[4] J. A. GAIDOS,[8] S. GAMMELL,[10] K. GIBBS,[1] G. H. GILLANDERS,[11] J. GRUBE,[3] J. HALL,[12]
T. A. HALL,[13] D. HANNA,[14] A. M. HILLAS,[3] J. HOLDER,[3] A. JARVIS,[7] M. JORDAN,[5] G. E. KENNY,[11] M. KERTZMAN,[15]
D. KIEDA,[12] J. KILDEA,[15] J. KNAPP,[3] K. KOSACK,[5] H. KRAWCZYNSKI,[5] F. KRENNRICH,[6] M. J. LANG,[11] S. LE BOHEC,[6]
E. LINTON,[4] J. LLOYD-EVANS,[3] A. MILOVANOVIC,[3] P. MORIARTY,[16] D. MULLER,[4] T. NAGAI,[12] S. NOLAN,[8]
R. A. ONG,[7] R. PALLASSINI,[3] D. PETRY,[17] B. POWER-MOONEY,[10] J. QUINN,[10] M. QUINN,[16] K. RAGAN,[14]
P. REBILLOT,[5] P. T. REYNOLDS,[18] H. J. ROSE,[3] M. SCHROEDTER,[1] G. H. SEMBROSKI,[8] S. P. SWORDY,[4]
A. SYSON,[3] V. V. VASSILIEV,[12] S. P. WAKELY,[4] G. WALKER,[12] T. C. WEEKES,[1] AND J. ZWEERINK[7]

ABSTRACT

We present results from observations of 29 BL Lacertae objects, taken with the Whipple Observatory 10 m gamma-ray telescope between 1995 and 2000. The observed objects are mostly at low redshift ($z < 0.2$), but observations of objects of up to $z = 0.444$ are also reported. Five of the objects are EGRET sources and two are unconfirmed TeV sources. Three of the confirmed sources of extragalactic TeV gamma rays were originally observed as part of this survey and have been reported elsewhere. No significant excesses are detected from any of the other objects observed, on timescales of days, months, or years. We report 99.9% confidence level flux upper limits for the objects for each observing season. The flux upper limits are typically 20% of the Crab flux, although for some sources, limits as sensitive as 6% of the Crab flux were derived. The results are consistent with the synchrotron self-Compton model predictions considered in this work.

Subject headings: BL Lacertae objects: general — galaxies: jets — gamma rays: observations

1. INTRODUCTION

BL Lacertae objects are members of the blazar class of active galactic nuclei (AGNs). Like all blazars, they exhibit rapid, large-amplitude variability at all wavelengths, high optical and radio polarization, and in some cases, apparent superluminal motion and/or gamma-ray emission. All of these observational properties lead to the widely held belief that blazars are AGNs with jets oriented nearly along our line of sight (Urry & Padovani 1995). The broadband spectral energy distribution (SED) of blazars, when plotted as νF_ν versus frequency, shows a double-peaked shape, with a smooth extension from radio to between IR and X-ray frequencies (depending on the specific blazar type), followed by a distribution that typically starts in the X-ray band and can peak in the gamma-ray band at energies as high as several hundred GeV. EGRET has detected more than 65 blazars (Hartman et al. 1999), 14 of which have been identified as BL Lac objects (Dermer & Davis 2000).

The low-energy part of the blazar SED is believed to be incoherent synchrotron radiation from a relativistic electron-positron plasma in the blazar jet. The origin of the high-energy emission is still a matter of considerable debate (e.g., Buckley 1998; Mannheim 1998). Leptonic models are the most popular models used to explain the observed gamma-ray emission from blazars. In synchrotron self-Compton (SSC) models, the gamma rays are produced through inverse Compton scattering of low-energy photons by the same electrons that produce the synchrotron emission at lower energies (Königl 1981; Maraschi, Ghisellini, & Celotti 1992; Dermer, Schlickeiser, & Mastichiadis 1992; Sikora, Begelman, & Rees 1994; Bloom & Marscher 1996; Sikora & Madejski 2001). In external Compton models, the dominant source of seed photons for upscattering in the inverse Compton process are ambient photons from the central accretion flow, the accretion disk, the broad-line region, the torus, the local infrared background, or some combination of these (Sikora et al. 1994; Dermer & Schlickeiser 1993; Blandford & Levinson 1995; Ghisellini & Madau 1996; Wagner et al. 1995). Another set of models

[1] Fred Lawrence Whipple Observatory, Harvard-Smithsonian Center for Astrophysics, P.O. Box 97, Amado, AZ 85645-0097; dhoran@cfa.harvard.edu.

[2] Physics Department, Tanta University, Tanta, Egypt.

[3] Department of Physics, University of Leeds, Leeds LS2 9JT, Yorkshire, England, UK.

[4] Enrico Fermi Institute, University of Chicago, Chicago, IL 60637.

[5] Department of Physics, Washington University, St. Louis, MO 63130.

[6] Department of Physics and Astronomy, Iowa State University, Ames, IA 50011-3160.

[7] Department of Physics, University of California, Los Angeles, CA 90095-1562.

[8] Department of Physics, Purdue University, West Lafayette, IN 47907.

[9] Department of Physics, Grinnell College, Grinnell, IA 50112-1690.

[10] Experimental Physics Department, National University of Ireland, Belfield, Dublin 4, Ireland.

[11] Department of Physics, National University of Ireland, Galway, Ireland.

[12] High Energy Astrophysics Institute, University of Utah, Salt Lake City, UT 84112.

[13] Department of Physics and Astronomy, University of Arkansas, Little Rock, AR 72204-1099.

[14] Physics Department, McGill University, Montreal, QC H3A 2T8, Canada.

[15] Department of Physics and Astronomy, DePauw University, Greencastle, IN 46135-0037.

[16] School of Science, Galway-Mayo Institute of Technology, Galway, Ireland.

[17] University of Maryland, Baltimore County, and NASA Goddard Space Flight Center.

[18] Department of Applied Physics and Instrumentation, Cork Institute of Technology, Cork, Ireland.

proposes that the gamma rays are the result of ultra–high energy ($E \gtrsim 10^{19}$ eV) protons producing TeV gamma rays as proton synchrotron radiation (Aharonian et al. 2000), in proton-induced electromagnetic cascades (Mannheim 1998), or by a combination of both processes (Mücke et al. 2003).

Among blazars, BL Lac objects are believed to be the best candidates for TeV emission. They have weak or absent optical emission lines, indicating that they may have less TeV-absorbing material near the emission region (Dermer & Schlickeiser 1994). Although they show relatively low luminosities compared to flat-spectrum radio quasars (FSRQs) and optically violent variables (OVVs), their SEDs peak at higher energies (Fossati et al. 1998). In blazar unification models in which electrons are assumed to be the progenitors of the gamma rays (e.g., Ghisellini et al. 1998), the lower luminosity of the BL Lac objects relative to the FSRQs implies that in BL Lac objects, electrons are cooled less efficiently. This means that the electrons reach higher energies and that the emitted gamma rays will therefore also be of higher energy.

Consistent with these expectations, BL Lac objects are the only type of blazars detected at very high energies (VHEs; $E \gtrsim 250$ GeV). Currently, six BL Lac objects are confirmed sources of VHE gamma rays. These include Mrk 421 (Punch et al. 1992), Mrk 501 (Quinn et al. 1996), H1426+428 (Horan et al. 2002), and 1ES 1959+650 (Nishiyama et al. 1999). The original detection of the nearby BL Lac object 1ES 2344+514 (Catanese et al. 1998) was confirmed by the HEGRA group (Tluczykont et al. 2003), while that of the Southern Hemisphere BL Lac object PKS 2155−304 (Chadwick et al. 1999) was confirmed recently by HESS (Djannati-Atai et al. 2003). Unconfirmed detections have been reported for the BL Lac objects 3C 66A (Neshpor et al. 1998) and BL Lacertae (Neshpor et al. 2001). The TeV blazars 1ES 2344+514, H1426+428, and 1ES 1959+650 were originally observed at Whipple as part of the BL Lac survey described here. Since they were detected during these observations, the results are described in detail elsewhere (Catanese et al. 1998; Horan et al. 2002; Holder et al. 2003) and are summarized here.

Padovani & Giommi (1995a) introduced the terminology "low-frequency–peaked BL Lac objects" (LBLs) to describe those BL Lac objects in which the lower energy SED peak occurs in the radio band and "high-frequency–peaked BL Lac objects" (HBLs) for those whose lower energy peak occurs in the X-ray band. Recently, deeper BL Lac surveys (e.g., Perlman et al. 1998; Laurent-Muehleisen et al., 1999; Caccianiga et al. 1999) have revealed evidence for the existence of BL Lac objects with properties intermediate to those in the LBL and HBL classes. Indeed, W Comae has recently been classified as an intermediate BL Lac object (Tagliaferri et al. 2000). This suggests that rather than being separate subclasses, LBLs and HBLs represent the edges of a sequence of progressively different BL Lac objects. The term "extreme blazars" was introduced by Ghisellini (1999) to describe those BL Lac objects whose first peak extends into the hard X-ray band. Such objects, which lie at the end of the "blazar sequence" proposed by Fossati et al. (1997), are good candidates for TeV emission since the second peak in their SEDs also lies at higher energies, meaning that they can be powerful at TeV energies.

With the exception of 3C 66A and BL Lacertae, all of the claimed and confirmed TeV gamma-ray emitting BL Lac objects are HBLs. H1426+428, Mrk 501, 1ES 2344+514, and, to a lesser extent, 1ES 1959+650 all have very hard X-ray energy spectra and fall into the class of extreme blazars. All of the TeV blazars but these four were listed as detections in the Third EGRET Catalog (Hartman et al. 1999). The second peak in the SED of these and other extreme objects can be studied in detail only at TeV energies since it lies above 100 GeV, where EGRET and *GLAST* are less sensitive. Ground-based gamma-ray telescopes therefore offer a unique opportunity to study this class of higher peaked blazars. Indeed, the majority of blazars detected by EGRET were FSRQs whose second SED peak falls in the MeV to GeV band.

In order to improve our understanding of the gamma-ray emission from BL Lac objects, we need to detect more of these objects at very high energies. Several groups have published upper limits on VHE emission from BL Lac objects in the last several years (Roberts et al. 1998, 1999; Chadwick et al. 1999; Aharonian et al. 2000), including the VERITAS collaboration (Kerrick et al. 1995), but these efforts have been on smaller groups of objects or not directed specifically at BL Lac objects. In this paper we present the results of our BL Lac observing program from 1995 January to 2000 July. The database comprises observations of 29 objects totaling 143 hr. We present the results of searches for emission spanning timescales of 30 minutes to 6 yr. No statistically significant excess emission above the background is found, and we discuss the implications of the nondetections.

These results supersede preliminary analyses presented in conference proceedings (Catanese et al. 1997a; Horan et al. 2000, 2004). Five of the objects presented here were later observed more intensively as part of an HBL observation program carried out by de la Calle Perez et al. (2003). In that survey, eight HBLs, selected from a list of TeV candidate objects derived by Costamante & Ghisellini (2002), were subjected to intensive Whipple observations during 2001 and 2002. These objects were all predicted to be VHE emitters based on the location of their synchrotron peak and on their high-density seed photons for the inverse Compton process. No evidence for TeV emission from these objects was found during this intensive monitoring campaign (de la Calle Perez et al. 2003).

2. SOURCE LIST

Table 1 lists the objects whose observations are reported here. In this table we provide the object's name (or names), equatorial coordinates, redshift, and classification. The locations of these BL Lac objects, along with those of 1ES 2344+514, H1426+428, and 1ES 1959+650, are plotted in Galactic coordinates in Figure 1.

The majority of the objects in Table 1 were selected for observations as part of three BL Lac campaigns. The first was a survey of all known (circa 1995) BL Lac objects with redshifts of $\lesssim 0.1$. The goal was to investigate the intrinsic characteristics of BL Lac objects that lead to the production of TeV gamma rays. We selected low-redshift objects to minimize the effect of the attenuation of the VHE gamma-ray signal by pair production with extragalactic background light (EBL; Stecker 1999; Primack et al. 1999; Vassiliev 2000) so that the intrinsic features could be compared. The second campaign was to search for TeV emission from HBLs in the redshift range from 0.1 to 0.2. We believed that because the HBLs have SEDs similar to the confirmed TeV emitters, they would be stronger TeV candidates than the LBLs. Because of the potential attenuation by the EBL and the larger pool of objects in the $z = 0.1$–0.2 range, we needed to be more selective in our surveys. The third campaign was a "snapshot survey" (D'Vali et al. 1999) in which many BL Lac objects that were considered likely candidates for TeV emission on the

TABLE 1
Observed BL Lac Objects

Name	R.A. (J2000.0)	Decl. (J2000.0)	z	Class[a]
1ES 0033+595	00 35 52.6	+59 50 05	0.086	HBL
1ES 0145+138	01 48 29.7	+14 02 18	0.125	HBL
RGB J0214+517	02 14 17.9	+51 44 52	0.049	HBL
3C 66A, 1ES 0219+428[b,c]...........................	02 22 39.6	+43 02 08	0.444	LBL
1ES 0229+200	02 32 48.4	+20 17 16	0.140	HBL
1H 0323+022, 1ES 0323+022	03 26 14.0	+02 25 15	0.147	HBL
EXO 0706.1+5913, RGB J0710+591	07 10 30.0	+59 08 20	0.125	HBL
1ES 0806+524	08 09 49.1	+52 18 59	0.138	HBL
PKS 0829+046, RGB J0831+044[c]...............	08 31 48.9	+04 29 39	0.180	LBL
1ES 0927+500	09 30 37.6	+49 50 26	0.188	HBL
S4 0954+65, RGB J0958+655[c]...................	09 58 47.2	+65 33 55	0.368	LBL
1ES 1028+511	10 31 18.4	+50 53 36	0.361	HBL
1ES 1118+424	11 20 48.0	+42 12 12	0.124	HBL
Mrk 40	11 25 36.2	+54 22 57	0.021	HBL
Mrk 180, 1ES 1133+704...........................	11 36 26.4	+70 09 27	0.045	HBL
1ES 1212+078	12 15 10.9	+07 32 04	0.130	HBL
ON 325, 1ES 1215+303	12 17 52.1	+30 07 01	0.130	LBL
1H 1219+301, 1ES 1218+304	12 21 21.9	+30 10 37	0.182	HBL
W Comae, 1ES 1218+285[c].........................	12 21 31.7	+28 13 59	0.102	LBL
MS 1229.2+6430, RGB J1231+642	12 31 31.4	+64 14 18	0.170	HBL
1ES 1239+069	12 41 48.3	+06 36 01	0.150	HBL
1ES 1255+244	12 57 31.9	+24 12 40	0.141	HBL
OQ 530, RGB J1419+543...........................	14 19 46.6	+54 23 15	0.151	LBL
4U 1722+11, RGB J1725+118[d]...................	17 25 04.3	+11 52 15	0.018	HBL
I Zw 187, 1ES 1727+502...........................	17 28 18.6	+50 13 10	0.055	HBL
1ES 1741+196	17 43 57.8	+19 35 09	0.084	HBL
3C 371, 1ES 1807+698..............................	18 06 50.6	+69 49 28	0.051	LBL
BL Lacertae, 1ES 2200+420[c]......................	22 02 43.3	+42 16 40	0.069	LBL
1ES 2321+419	23 23 52.1	+42 10 59	0.059	HBL

Note.—Units of right ascension are hours, minutes, and seconds, and units of declination are degrees, arcminutes, and arcseconds.

[a] HBL = high-frequency–peaked BL Lac object; LBL = low-frequency–peaked BL Lac object.
[b] Unconfirmed source of TeV gamma rays.
[c] EGRET source of >100 MeV gamma rays.
[d] This object is sometimes quoted as having a redshift of 0.018. However, this is based on one absorption line (Veron-Cetty & Veron 1993), and the object is more commonly listed as having an unknown redshift.

basis of the same criteria as the second survey were observed. When in a flaring state, a 10 minute observation of Mrk 421 or Mrk 501 was enough to achieve a significant detection. The selected snapshot survey targets were therefore observed for 10 minutes each on a regular basis in the hope of catching one of them in such a flaring state. The objects were grouped based on their proximity to each other on the celestial sphere. Objects in each group were then observed consecutively so as to minimize telescope slewing time. The remaining objects with known redshift were chosen because they were EGRET sources (W Comae, PKS 0829+046, S4 0954+65, 3C 66A) or because they were a superluminal source (OQ 530). RGB J1725+118 (4U 1722+11) was observed because one mea-surement (Veron-Cetty & Veron 1993) derived a redshift of $z = 0.018$, which would make it the closest known BL Lac object. The estimate was, however, derived from one ab-sorption line, and many papers list its redshift as unknown (e.g., Padovani & Giommi 1995b).

3. ANALYSIS METHODS

3.1. Telescope Configurations

The VHE observations reported in this paper were made with the atmospheric Cerenkov imaging technique (Cawley &

Weekes 1995; Reynolds et al. 1993) using the 10 m optical reflector located at the Whipple Observatory on Mount Hopkins in Arizona (elevation 2.3 km; Cawley et al. 1990). A camera, consisting of an array of photomultiplier tubes (PMTs) mounted in the focal plane of the reflector, records images of atmospheric Cerenkov radiation from air showers produced by gamma rays and cosmic rays. The observations reported here span 5 yr, and the camera of the Whipple gamma-ray telescope changed several times during that period. Table 2 outlines the configurations of the camera. Light concentrators are reflective cones that are mounted in front of the PMTs to improve light collection efficiency and reduce albedo. During 1999, an intelligent trigger, the "pattern se-lection trigger" (PST; Bradbury et al. 1999), which required three adjacent tubes to record a signal above a certain level within a preset window, was installed. Prior to this, a trigger was declared if any two PMTs in the camera recorded a signal above a certain level within a preset window. The PST reduces the number of triggers caused by fluctuations of the night-sky background and thus allows the telescope to operate at lower energies. The mirror reflectivity and trigger settings also changed over time. Each observing season runs approximately from September through June. Observations are not usually carried out in July and August because the monsoon season,
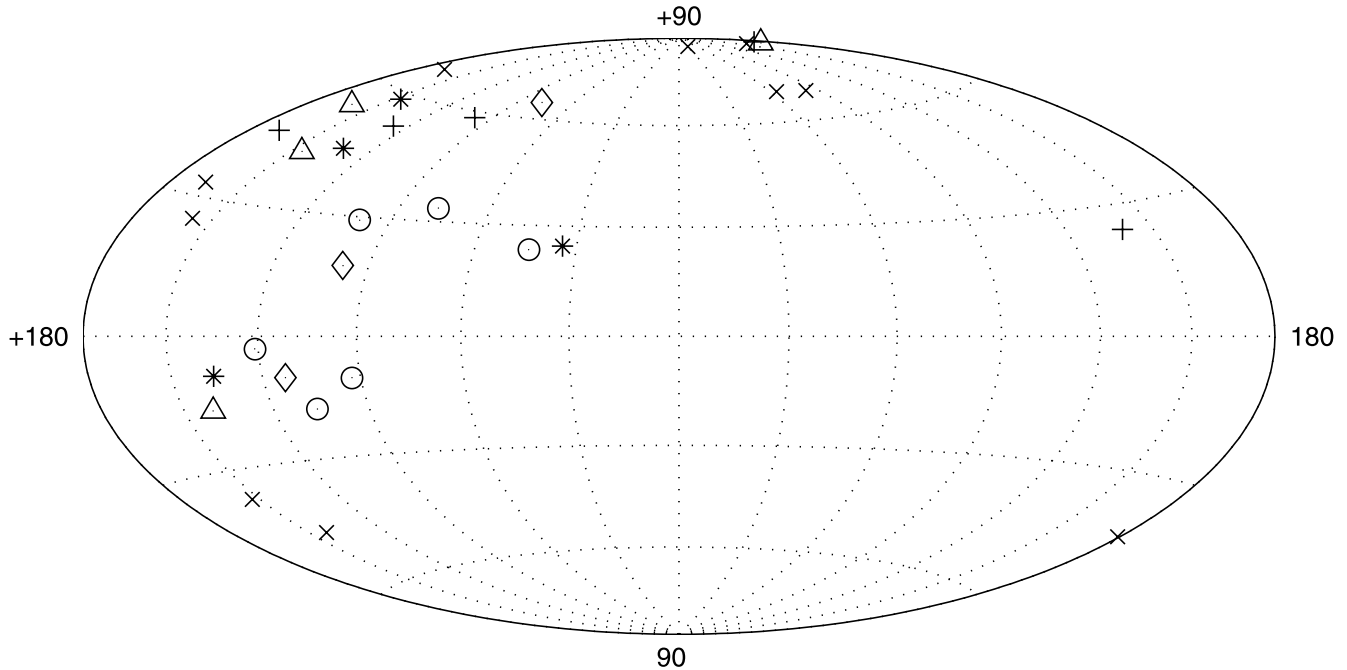
Fig. 1.—Locations of the 32 BL Lac objects originally observed as part of this survey are plotted in Galactic coordinates. The three objects that were subsequently detected (1ES 2344, H1426+428, and 1ES 1959+650) are labeled with diamonds, while the 29 objects whose upper limits are reported here are labeled according to their redshift. The stars mark the four objects lying at $z < 0.05$, the circles mark six objects lying between $z = 0.05$ and 0.1, the crosses mark the 10 objects lying between $z = 0.1$ and 0.15, the plus symbols mark the five objects lying between $z = 0.15$ and 0.20, and the triangles mark the four objects that lie at $z > 0.20$.

during which lightning storms strike frequently, occurs at this time.

3.2. *Gamma-Ray Selection*

We characterize each Cerenkov image using a moment analysis (Reynolds et al. 1993). The roughly elliptical shape of the image is described by the parameters "length" and "width," and its location and orientation within the telescope field of view are given by the parameters "distance" and α, respectively. We also determine the two highest signals recorded by the PMTs ("max1" and "max2") and the amount of light in the image "size." In addition, we can apply a cut on the third moment parameter "asymmetry" to select gamma-ray candidates, since the narrower tail of the image should point back toward the source location within the field of view. The α-parameter tests whether the major axis of the image is aligned with the putative source location; it does not eliminate events whose major axes are parallel with the source location but whose image points away from it. The asymmetry

parameter is not an efficient cut for cameras with small fields of view because the images are often truncated.

Because of the changes in the camera discussed above in § 3.1, the optimum cuts for selecting gamma rays change with time. The cuts for different camera configurations are listed in Table 3. They result in different sensitivities, energy ranges, and effective areas for each camera. This limits our ability to combine data from different observing periods into single upper limits. Given the variable nature of BL Lac objects, however, deriving single upper limits for several years of observation is of dubious benefit. Instead, we quote upper limits for each observing period.

3.3. *Tracking Analysis*

The observations presented here were all taken in the Tracking data collection mode wherein only the on-source position is tracked, in runs of 28 minutes' duration. To estimate the expected background, we use those events that pass all of the gamma-ray selection criteria except orientation

TABLE 2

WHIPPLE CAMERA CONFIGURATIONS

Parameter	1995 January–1996 December	1997 January–1997 June	1997 September–1998 December	1998 December–1999 March	1999 October–2000 July
Number of PMTs.............	109	151	331	331	379[a]
PMT spacing (deg)	0.259	0.259	0.24	0.24	0.12
Field of view (deg)..........	3	3.3	4.8	4.8	2.6
Light concentrators	Yes	Yes	No	Yes	Yes
Pattern trigger	No	No	No	No	Yes

[a] The camera consists of 379 inner tubes with field of view of $0°\!.12$ diameter surrounded by three circular rings of PMTs (111 in all) with field of view of $0°\!.26$ diameter. The outer rings of tubes were not used in this analysis, and so the parameters presented here pertain only to the inner 379 tubes.

TABLE 3
Analysis Cuts

Parameter	1995 January– 1996 December	1997 January– 1997 June	1997 September– 1998 December	1998 December– 1999 March	1999 October– 2000 July
max1[a]	>100	>95	>60	>60	>30
max2[a]	>80	>45	>40	>40	>30
Size[a]	>400	NA[b]	NA	NA	NA
Length (deg)	>0.16, <0.30	>0.16, <0.33	>0.16, <0.50	>0.16, <0.50	>0.13, <0.25
Width (deg)	>0.073, <0.15	>0.073, <0.16	>0.073, <0.16	>0.073, <0.16	>0.05, <0.12
Distance (deg)	>0.51, <1.10	>0.51, <1.17	>0.51, <1.55	>0.51, <1.55	>0.40, <1.00
α (deg)	<15	<15	<15	<15	<15
Asymmetry (deg)	NA	>0	>0	>0	>0
Length over size	NA	NA	NA	NA	<0.0004

[a] Quantities are in units of digital counts; 1 digital count $\approx$ 1 photoelectron.
[b] NA means the cut was not applied.

(characterized by the α-parameter). We use events with values of α between $20°$ and $65°$ as the background region and convert the counts to an estimated background within the on-source region ($\alpha < 10°$ or $15°$; see Table 3) by multiplying the number of counts by a ratio determined from observations of non–source regions taken at other times during the observing season. This method has been described in detail by Catanese et al. (1998). The value of the factor that converts the off-source counts to an on-source background estimate varies with season because of changes in the camera sensitivity and field of view. The estimated values for each of the observing periods are listed in Table 4.

In the case of tracking analysis, to establish the significance (S) of an excess or of a deficit, we use simple error propagation:

$$S = \frac{N_{on} - rN_{bkd}}{\sqrt{N_{on} + r^2 N_{bkd} + N_{bkd}^2 (\Delta r)^2}}, \quad (1)$$

where N_{on} is the number of events in the on-source region (designated by the α-cut in Table 3), N_{bkd} is the number of events in the background region ($\alpha = 20°$–$65°$), and $r \pm \Delta r$ is the tracking ratio and its statistical uncertainty.

3.4. Flux Upper Limit Estimation

After we select gamma-ray candidate events, we determine the significance of any excess or deficit in the observations. If the excess or the deficit is not statistically significant, as is the case for all observations reported here, we calculate a 99.9% confidence level upper limit on the count rate by using the method of Helene (1983). To convert these flux upper limits to absolute fluxes, we first express them as a fraction of the Crab Nebula count rate by using observations from the same observing period. Although this method assumes a Crab-like spectrum for the BL Lac objects, it corrects for season-to-season variations in factors such as PMT gain and mirror reflectivity that affect the telescope response and therefore its gamma-ray count rate. The count rates observed for the Crab Nebula for the observing periods reported here are given in Table 4. Analysis of the Crab Nebula data shows that for runs taken under good weather conditions, the gamma-ray count rate does not change significantly within a season (Quinn 1998). We can therefore assume that the gamma-ray count rate for a source can be reliably expressed in terms of the Crab Nebula flux over the course of the season.

Once we have the flux limit expressed as a fraction of the Crab Nebula count rate, we multiply it by the integral Crab Nebula flux (in units of photons cm^{-2} s^{-1}) above the peak response energy of the observations (E_p). We define E_p as the energy at which the collection area folded with an $E^{-2.5}$ spectrum, that of the Crab Nebula (Hillas et al. 1998), reaches a maximum. The integral fluxes from the Crab Nebula above E_p for the different observation periods reported here are given in Table 4. Upper limits are an estimate of the flux that could be present in the data set but not produce a significant excess. This is most accurately derived from the count rate because that is what determines the statistical significance of the excess. The Crab Nebula count rate and flux uncertainties affect only the normalization, so the flux upper limits quoted in terms of photons cm^{-2} s^{-1} have an uncertainty of ~25%, mainly from the uncertainty in the Crab Nebula photon flux.

TABLE 4
Analysis Parameters

Period	Tracking Ratio	Crab Rate (γ minute^{-1})	Peak Response Energy (GeV)	Integral Crab Flux[a]
1995 Jan–Aug	0.292 ± 0.005	2.08 ± 0.15	300	1.26
1995 Oct–1996 Jul	0.292 ± 0.004	1.58 ± 0.05	350	1.05
1996 Oct–Dec	0.316 ± 0.004	1.69 ± 0.07	350	1.05
1997 Jan–Jun	0.345 ± 0.005	2.30 ± 0.10	350	1.05
1998 Jan–Dec	0.366 ± 0.002	1.94 ± 0.15	500	0.60
1998 Dec–1999 Mar	0.367 ± 0.004	2.62 ± 0.26	400	0.84
1999 Oct–2000 Jul	0.312 ± 0.002	2.64 ± 0.12	430	0.76

[a] Fluxes are quoted in units of 10^{-10} photons cm^{-2} s^{-1} above the corresponding peak response energy.

TABLE 5

THE OBSERVATION RESULTS FOR EACH OBJECT, FOR EACH OBSERVING PERIOD DURING WHICH IT WAS OBSERVED

		EXPOSURE		MAXIMUM σ		FLUX	FLUX
OBJECT	OBSERVATION PERIOD	(hr)	σ	Month	Night	(c.u.)	(f.u.)
1ES 0033+595	1995 Dec	1.85	−0.59	−0.59	0.19	< 0.200	< 2.10
1ES 0145+138	1996 Oct–1996 Nov	7.85	−1.01	0.08	1.77	< 0.093	< 0.98
	1998 Nov–1998 Dec	2.29	0.22	0.63	0.63	< 0.512	< 3.50
	1998 Dec–1999 Jan	1.98	−0.50	0.38	1.31	< 0.357	< 3.34
RGB J0214+517	1999 Dec–2000 Jan	6.01	0.29	0.36	1.58	< 0.165	< 1.45
3C 66A.......................	1995 Oct–1995 Nov	8.00	−2.00	−1.18	0.82	< 0.056	< 0.59
1ES 0229+200	1996 Nov–1996 Dec	7.85	0.15	0.57	1.37	< 0.113	< 1.19
	1998 Nov–1998 Dec	2.30	−1.08	−0.78	0.48	< 0.326	< 2.23
	1998 Dec–1999 Jan	1.78	−0.40	0.66	0.74	< 0.403	< 3.76
1H 0323+022	1996 Nov–1996 Dec	10.18	1.02	1.02	1.96	< 0.181	< 1.90
	1997 Jan	0.91	0.20	0.20	0.20	< 0.298	< 3.13
	1998 Dec–1999 Jan	3.18	1.69	1.73	1.85	< 0.509	< 4.75
EXO 0706.1+5913.....	1996 Dec	5.55	−1.16	−1.16	0.17	< 0.087	< 0.91
	1997 Jan–1997 Mar	3.69	0.76	0.79	1.46	< 0.161	< 1.69
	1998 Nov	1.83	−0.40	−0.40	1.49	< 0.524	< 3.58
	1998 Dec–1999 Feb	1.90	0.07	1.36	1.71	< 0.459	< 4.29
1ES 0806+524	1996 Feb–1996 Mar	5.57	0.46	0.52	1.04	< 0.104	< 1.09
	2000 Jan–2000 Mar	4.16	−0.29	0.69	0.69	< 1.293	< 11.4
PKS 0829+046..........	1995 Jan–1995 Apr	11.07	1.25	1.73	3.14	< 0.117	< 1.47
1ES 0927+500	1996 Dec	5.08	−1.92	−1.92	0.39	< 0.064	< 0.67
	1997 Jan–1997 Apr	5.04	−1.03	0.22	1.23	< 0.076	< 0.80
S4 0954+65................	1995 Feb–1995 Mar	3.70	−1.09	−0.50	−0.11	< 0.096	< 1.21
1ES 1028+511	1998 Dec–1999 Feb	4.43	0.57	1.36	2.03	< 0.287	< 2.68
1ES 1118+424............	1998 Feb–1998 Apr	7.30	−0.25	1.29	1.80	< 0.218	< 1.49
	1998 Dec–1999 Feb	3.60	0.27	1.04	1.81	< 0.310	< 2.90
	2000 Jan–2000 May	6.97	−0.62	1.29	1.61	< 0.116	< 1.02
Mrk 40	2000 Jan–2000 Apr	10.16	2.59	1.66	1.56	< 0.206	< 1.81
Mrk 180	1995 Jan–1995 Apr	5.55	−0.10	0.45	1.07	< 0.108	< 1.36
	1995 Dec–1996 May	20.46	−0.26	1.01	1.70	< 0.105	< 1.10
	1997 Jan	0.79	−0.17	−0.17	−0.17	< 0.303	< 3.18
1ES 1212+078	1999 Feb	1.13	0.44	0.44	1.83	< 0.778	< 7.26
	2000 Jan–2000 May	3.70	1.30	1.52	1.73	< 0.321	< 2.82
ON 325	1999 Feb	0.97	1.27	1.27	1.20	< 0.882	< 8.23
	2000 Jan–2000 May	5.05	0.88	1.94	1.62	< 0.215	< 1.89
1H 1219+301	1995 Jan–1995 May	2.77	2.71	2.90	2.95	< 0.226	< 2.85
	1997 Feb–1997 Jun	11.27	0.99	1.55	1.97	< 0.079	< 0.83
	1998 Jan–1998 Mar	1.38	−1.96	−1.27	−0.32	< 0.356	< 2.43
	1998 Dec–1999 Feb	2.94	−0.08	0.48	0.88	< 0.296	< 2.77
	2000 Jan–2000 Apr	3.69	0.04	1.48	1.18	< 0.191	< 1.68
W Comae	1995 Feb–1995 Apr	14.33	−0.57	−0.11	1.14	< 0.052	< 0.66
	1996 Jan–1996 May	15.73	−0.29	0.24	1.38	< 0.055	< 0.58
	1999 Jan–1999 Feb	4.43	−0.03	0.58	1.91	< 0.312	< 2.92
	2000 Jan–2000 Apr	4.72	−0.58	1.01	1.76	< 0.148	< 1.30
MS 1229.2+6430	1995 Feb–1995 Apr	1.39	1.32	1.08	1.08	< 0.286	< 3.60
	1999 Feb	2.04	−0.76	−0.76	1.18	< 0.446	< 4.16
	2000 Jan–2000 May	6.01	0.35	1.72	1.72	< 0.170	< 1.50
1ES 1239+069	1999 Jan–1999 Feb	1.73	0.78	0.69	1.74	< 0.616	< 6.04
	2000 Jan–2000 May	5.08	0.11	1.19	1.42	< 0.197	< 1.73
1ES 1255+244	1997 Feb–1997 May	5.54	1.19	1.01	1.35	< 0.112	< 1.18
	1998 Mar	0.46	0.13	0.13	0.13	< 1.112	< 7.60
	1999 Feb	1.73	0.15	0.15	1.10	< 0.508	< 4.75
	2000 Jan–2000 May	4.16	−0.54	1.30	1.41	< 0.164	< 1.45
OQ 530	1995 Mar–1995 May	7.39	−0.73	−0.15	0.76	< 0.058	< 0.73
4U 1722+11	1995 Apr–1995 May	2.77	−0.08	0.28	0.70	< 0.124	< 1.56
I Zw 187	1995 Mar–1995 Apr	2.31	−1.27	−0.07	0.63	< 0.086	< 1.08
	1996 Apr–1996 May	2.32	0.61	0.85	1.19	< 0.150	< 1.58
1ES 1741+196	1996 May–1996 Jul	9.23	−1.02	0.46	2.07	< 0.053	< 0.56
	1998 May	0.46	−0.08	−0.08	−0.08	< 1.168	< 7.99
3C 371	1995 May–1995 Jun	13.04	0.41	0.41	1.68	< 0.190	< 1.23
BL Lacertae...............	1995 Jul	4.62	1.07	1.09	1.09	< 0.109	< 1.37
	1995 Oct–1995 Nov	39.09	−1.48	−0.21	0.85	< 0.038	< 0.40
	1998 May–1998 Jun	0.92	0.47	0.71	0.71	< 1.722	< 8.02
1ES 2321+419	1995 Oct–1995 Nov	6.42	−1.07	1.50	1.50	< 0.101	< 1.06

NOTES.—For each BL Lac object, the total combined significance for each period is given along with the maximum statistical significance seen over any one night and any month during that period. The flux upper limits are also presented for each observing period both in absolute terms (flux units, f.u., 10^{-11} ergs cm^{-2} s^{-1}) and in Crab units (c.u.).

4. RESULTS AND DISCUSSION

Table 5 summarizes the results of the observations of the BL Lac objects observed but not detected between 1995 January and 2000 July, while Table 6 summarizes the results of the observations taken of H1426+428, 1ES 1959+650, and 1ES 2344+514, the three BL Lac objects that were detected during this survey. For each target object, we list the observation exposure during each season, the significance of the excess or deficit of these observations, the maximum significances for a night or month of observations, and the flux upper limits expressed as fractions of the Crab count rate and in integral flux units (assuming a Crab-like spectrum). Many of the objects were observed over a number of different observing seasons, resulting in a range of upper limits above different values of E_p. No evidence for a statistically significant excess or deficit was seen in the detected count rate from any of the objects for any of the time periods examined. The distribution of the significances for each object for each observing season is shown in Figure 2. This distribution has a mean of 0.005 with a standard deviation of 0.976. The black curve shows the expected shape if the significances were drawn from a Gaussian distribution. The Kolmogorov-Smirnov test returns a 95% probability that the data are normally distributed.

Table 7 summarizes the detections of H1426+428, 1ES 1959+650, and 1ES 2344+514, the three target BL Lac objects that have been subsequently confirmed as TeV emitters.

In order to investigate how much the flux upper limits change if the spectral index is not the same as that of the Crab Nebula, estimates of the flux upper limits for the BL Lac objects were made assuming source spectral indexes of -2.2 and -2.8. The integral flux from the Crab Nebula above 300 GeV was used to scale the previously calculated upper limits. This integral flux was assumed to remain constant when the spectral index was changed; E_p was not adjusted to account for the response of the telescope to the different input spectra, but this effect should be very small. Table 8 lists the flux upper limits for each BL Lac object for each observing season when these different source spectral indexes were assumed.

Costamante & Ghisellini (2002) have made predictions for the TeV flux from 14 of the BL Lac objects included in this paper using two different methods. In the first, an SSC model was used to fit the multiwavelength data gathered on each of the objects, while in the second approach a phenomenological description of the average SED of the blazars was derived on
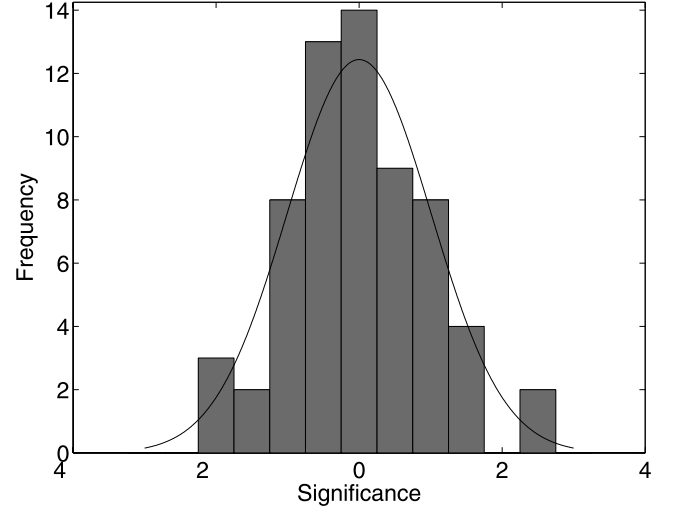

Fig. 2.—Significance of the deficit or excess in the detected count rate from each of the 29 BL Lac objects for each season during which they were observed. This distribution has a mean of 0.005 and standard deviation of 0.976. The black curve shows the expected shape if the significances were normally distributed. This curve fits the data at the 95% confidence level.

the basis of their observed bolometric luminosity (Fossati et al. 1998). The resulting flux predictions from each of the two methods were given above 300 GeV and above 1 TeV. In order to compare the upper limits presented here with these predictions, our upper limits that were not already derived above 300 GeV were extrapolated to this energy. This was done by first expressing the flux upper limit as a fraction of the Crab flux at that energy, $F_{\mathrm{BL\,Lac}}(>E_p)$. This was then scaled to 300 GeV assuming a Crab-like spectrum. Thus, an upper limit on the integral flux for each BL Lac object above 300 GeV for each observing season, $F_{\mathrm{BL\,Lac}}(>300\ \mathrm{GeV})$, was calculated:

$$F_{\mathrm{BL\,Lac}}(>300\ \mathrm{GeV}) = F_{\mathrm{BL\,Lac}}(>E_p)\,F_{\mathrm{Crab}}(>E_p)\left(\frac{300}{E_p}\right)^{-1.5}; \quad (2)$$

$F_{\mathrm{Crab}}(>E_p)$ is the integral flux from the Crab Nebula above E_p in units of photons cm^{-2} s^{-1}, assuming an integral spectral index of -1.5; $F_{\mathrm{BL\,Lac}}(>E_p)$ is the upper limit on the flux from the BL Lac object above E_p expressed as a fraction of the Crab Nebula integral flux at this energy.

TABLE 6
Observation Results for the Three Detected BL Lac Objects That Were
Originally Observed as Part of This Survey

| | | Exposure | | Maximum σ | | Flux |
Object	Observation Period	(hr)	σ	Month	Night	(f.u.)
H1426+428	1995 Jun–1995 Jul	3.48	2.11	2.11	2.05	< 0.2
	1997 Feb–1997 Jun	13.16	1.70	2.18	1.62	< 0.1
	1998 Apr	0.87	1.70	1.70	1.99	< 6.7
1ES 1959+650	1995 Jun	7.21	1.02	0.93	1.17	< 1.4
	1996 May–1996 Jul	3.25	0.33	0.68	1.10	< 1.5
	1998 Jul	0.16	−0.11	−0.11	−0.11	< 12.6
1ES 2344+514	1995 Oct–1996 Jan	20.50	5.82	6.50	5.80	. . .[a]

Notes.—For each observing period during which the objects were observed, prior to detection, the total combined significance is given along with the maximum statistical significance seen over any one night and any month during that period. The flux upper limits are also presented for each observing period in absolute terms (flux units, f.u., 10^{-11} ergs cm^{-2} s^{-1}).
[a] 1ES 2344+514 was detected during the first observing season in which it was observed. See Table 7 for the details.

TABLE 7
SUMMARY OF THE DETECTIONS OF THE THREE OBJECTS DETECTED DURING THIS SURVEY

Object	Observing Season of Detection	Peak Response Energy (GeV)	Integral Flux	Detection Paper
H1426+428	2000 Oct–2001 Jul	280	2.0 ± 0.3	Horan et al. 2002
1ES 1959+650	2001 Oct–2002 Jul	600	. . .[a]	Holder et al. 2003
1ES 2344+514	1995 Oct–1996 Jul	350	1.1 ± 0.4	Catanese et al. 1998

NOTES.—The observing season during which the objects were detected, the peak response energy for that season, and, where available, the detection integral flux in units of 10^{-11} photons cm^{-2} s^{-1} above the corresponding peak response energy, along with a reference to the detection paper, are given for each object.

[a] No flux was quoted in the detection paper because of difficulties in performing a spectral analysis due to a decrease in telescope efficiency during the course of the observations.

When deriving their flux predictions, Costamante & Ghisellini (2002) did not take into account absorption of the gamma rays by the infrared background. The predictions above 300 GeV could therefore change by factors on the order of 5 for objects at redshifts above 0.2. The upper limits presented here were compared with these predictions, and those of four BL Lac objects, shown in Table 9, were found during all seasons in which they were observed to be lower than the predicted fluxes according to the Fossati approach (Fossati et al. 1998) adapted in Costamante & Ghisellini (2002). Those of two more BL Lac objects, also listed in Table 9, were found to be lower during some of the observing periods. All of the upper limits calculated were higher than the fluxes predicted using the one-zone SSC model (Costamante & Ghisellini 2002). It should be noted, however, that the upper limits quoted here pertain only to the specific period during which the observations were made. As demonstrated by Böttcher, Muckherjee, & Reimer (2002), spectral fitting of blazars is subject to very large uncertainties when nonsimultaneous multiwavelength data are used. Indeed, it is also shown that even with the best currently available simultaneous optical–X-ray data, there is a very wide range in the predicted fluxes above 40 GeV. Given an observed X-ray flux, the predicted gamma-ray flux depends very sensitively on the model parameters and, even for simultaneous data, can vary by large factors because of the uncertainty in these parameters.

In the absence of dedicated simultaneous multiwavelength data, it is difficult to use these data to constrain emission models. However, many of the objects surveyed here are monitored by the All Sky Monitor (ASM) on board the *Rossi X-Ray Timing Explorer* (*RXTE*). For many other TeV blazars, the soft X-ray flux has been seen to rise during periods when the gamma-ray flux was also high. For example, Mrk 501 was observed to have a higher than average flux in the ASM during 1997, the same year during which the greatest TeV flaring activity detected to date was observed (Catanese et al. 1997b; Quinn et al. 1999). In order to see if any of the BL Lac objects surveyed here were particularly active in the X-ray band during these observations, the X-ray curves for the objects presented here that are monitored by ASM were analyzed. If heightened X-ray activity were detected in the absence of corresponding gamma-ray activity, this could have interesting consequences for emission models. Out of the 29 objects presented here, 25 were monitored on a regular basis by the ASM. The nightly average light curves for each of these were generated. The flux from each object was found to be, on average, very low ($\lesssim 0.01$ Crab units) with no evidence for dramatic flaring or for any sustained period of X-ray activity.

Current and future observing campaigns at the Whipple Observatory make use of BL Lac monitoring at X-ray wavelengths to try to predict when an object might be in a higher flux state and thus detectable in the VHE band. Elevated gamma-ray fluxes are often accompanied by a corresponding increase in the X-ray flux (e.g., Maraschi et al. 1999; Jordan et al. 2001). Thus, by monitoring the X-ray activity from blazars, we can identify periods of increased activity during which the VHE flux may also be stronger. However, the relationship between the X-ray and gamma-ray flux has been shown to be complicated with gamma-ray flares being detected in the absence of X-ray flares (Holder et al. 2003; Krawczynski et al. 2003), and vice-versa (Rebillot et al. 2003).

Finally, it should be noted that although none of the objects presented here were found to have a statistically significant TeV flux during these observations, three of the confirmed TeV blazars were detected during this survey. When 1ES 2344+514, H1426+428, and 1ES 1959+650 were initially observed at Whipple, it was as part of this BL Lac campaign, and like the objects listed here, they were not detected. In subsequent years, however, continued monitoring with deeper exposures revealed these objects to be TeV emitters when in more active states, although not always detectable when in their quiescent state. Continued VHE observations of the BL Lac objects presented here, in particular those shown to have extreme properties (de la Calle Perez et al. 2003), accompanied by monitoring of their X-ray flux level, may reveal many more of them to be TeV emitters. Indeed, since extreme BL Lac objects, the best blazar candidates for TeV emission, have lower luminosity at all wavelengths than their lower energy peaked counterparts, their flux level often lies below the detection threshold of the current generation of imaging atmospheric Cerenkov telescopes when they are in quiescent state. As the next generation of ground-based gamma-ray telescopes come on line with their increased flux sensitivity, they will offer a unique opportunity to study this low-luminosity class of blazars and should detect many more of these objects.

Future X-ray all-sky monitor experiments like LOBSTER (Black et al. 2003) and EXIST (Grindlay et al. 2003), with their improved flux sensitivity and increased bandwidth, will allow for more detailed monitoring of the X-ray emission from blazars, thus providing valuable information that can be used to trigger observations at gamma-ray energies. These X-ray missions, coupled with the next generation of higher sensitivity VHE observatories such as VERITAS, HESS, MAGIC, and CANGAROO, should allow both lower power extreme BL Lac objects and lower frequency peaked blazars (LBLs and FSRQs) to be detected.

TABLE 8
Flux Upper Limits for Each Object

Object	Observation Period	Peak Response Energy	Flux (f.u.) $\alpha = -2.2$	$\alpha = -2.5$	$\alpha = -2.8$
1ES 0033+595	1995 Dec	350	<2.1476	<2.1000	<1.9579
1ES 0145+138	1996 Oct–1996 Nov	350	<1.0022	<0.9800	<0.9137
	1998 Nov–1998 Dec	500	< 4.0605	<3.5000	<2.9886
	1998 Dec–1999 Jan	400	<3.6323	<3.3400	<3.0565
RGB J0214+517	1999 Dec–2000 Jan	430	<1.6103	<1.4500	<1.2974
3C 66A..................	1995 Oct–1995 Nov	350	<0.6034	<0.5900	<0.5501
1ES 0229+200	1996 Nov–1996 Dec	350	<1.2170	<1.1900	<1.1095
	1998 Nov–1998 Dec	500	<2.5871	<2.2300	<1.9042
	1998 Dec–1999 Jan	400	<4.0891	<3.7600	<3.4408
1H 0323+022	1996 Nov–1996 Dec	350	<1.9431	<1.9000	<1.7714
	1997 Jan	350	<3.2010	<3.1300	<2.9182
	1998 Dec–1999 Jan	400	<5.1657	<4.7500	<4.3468
EXO 0706.1+5913............	1996 Dec	350	<0.9306	<0.9100	<0.8484
	1997 Jan–1997 Mar	350	<1.7283	<1.6900	<1.5756
	1998 Nov	500	<4.1533	<3.5800	<3.0569
	1998 Dec–1999 Feb	400	<4.6655	<4.2900	<3.9258
1ES 0806+524	1996 Feb–1996 Mar	350	<1.1147	<1.0900	<1.0162
	2000 Jan–2000 Mar	430	<12.6599	<11.4000	<10.2005
PKS 0829+046............	1995 Jan–1995 Apr	300	<1.4700	<1.4700	<1.4700
1ES 0927+500	1996 Dec	350	<0.6852	<0.6700	<0.6247
	1997 Jan–1997 Apr	350	<0.8181	<0.8000	<0.7459
S4 0954+65............	1995 Feb–1995 Mar	300	<1.2100	<1.2100	<1.2100
1ES 1028+511	1998 Dec–1999 Feb	400	<2.9146	<2.6800	<2.4525
1ES 1118+424............	1998 Feb–1998 Apr	500	<1.7286	<1.4900	<1.2723
	1998 Dec–1999 Feb	400	<3.1538	<2.9000	<2.6538
	2000 Jan–2000 May	430	<1.1327	<1.0200	<0.9127
Mrk 40	2000 Jan–2000 Apr	430	<2.0100	<1.8100	<1.6196
Mrk 180	1995 Jan–1995 Apr	300	<1.3600	<1.3600	<1.3600
	1995 Dec–1996 May	350	<1.1249	<1.1000	<1.0256
	1997 Jan	350	<3.2521	<3.1800	<2.9648
1ES 1212+078	1999 Feb	400	<7.8954	<7.2600	<6.6437
	2000 Jan–2000 May	430	<3.1317	<2.8200	<2.5233
ON 325	1999 Feb	400	<8.9503	<8.2300	<7.5314
	2000 Jan–2000 May	430	<2.0989	<1.8900	<1.6911
1H 1219+301	1995 Jan–1995 May	300	<2.8500	<2.8500	<2.8500
	1997 Feb–1997 Jun	350	<0.8488	<0.8300	<0.7738
	1998 Jan–1998 Mar	500	<2.8191	<2.4300	<2.0750
	1998 Dec–1999 Feb	400	<3.0124	<2.7700	<2.5349
	2000 Jan–2000 Apr	430	<1.8657	<1.6800	<1.5032
W Comae	1995 Feb–1995 Apr	300	<0.6600	<0.6600	<0.6600
	1996 Jan–1996 May	350	<0.5932	<0.5800	<0.5408
	1999 Jan–1999 Feb	400	<3.1756	<2.9200	<2.6721
	2000 Jan–2000 Apr	430	<1.4437	<1.3000	<1.1632
MS 1229.2+6430	1995 Feb–1995 Apr	300	<3.6000	<3.6000	<3.6000
	1999 Feb	400	<4.5241	<4.1600	<3.8069
	2000 Jan–2000 May	430	<1.6658	<1.5000	<1.3422
1ES 1239+069	1999 Jan–1999 Feb	400	<6.5686	<6.0400	<5.5273
	2000 Jan–2000 May	430	<1.9212	<1.7300	<1.5480
1ES 1255+244	1997 Feb–1997 May	350	<1.2068	<1.1800	<1.1001
	1998 Mar	500	<8.8171	<7.6000	<6.4896
	1999 Feb	400	<5.1657	<4.7500	<4.3468
	2000 Jan–2000 May	430	<1.6103	<1.4500	<1.2974
OQ 530	1995 Mar–1995 May	300	<0.7300	<0.7300	<0.7300
4U 1722+11	1995 Apr–1995 May	300	<1.5600	<1.5600	<1.5600
I Zw 187	1995 Mar–1995 Apr	300	<1.0800	<1.0800	<1.0800
	1996 Apr–1996 May	350	<1.6158	<1.5800	<1.4731
1ES 1741+196	1996 May–1996 Jul	350	<0.5727	<0.5600	<0.5221
	1998 May	500	<9.2695	<7.9900	<6.8226
3C 371	1995 May–1995 Jun	300	<1.2300	<1.2300	<1.2300
BL Lacertae............	1995 Jul	300	<1.3700	<1.3700	<1.3700
	1995 Oct–1995 Nov	350	<0.4091	<0.4000	<0.3729
	1998 May–1998 Jun	500	<9.3043	<8.0200	<6.8482
1ES 2321+419	1995 Oct–1995 Nov	350	<1.0840	<1.0600	<0.9883

Notes.—These are the flux upper limits for each object, for each observing period during which it was observed, when input spectra with different spectral indexes (α) were assumed. The flux upper limits are given in absolute terms (flux units, f.u., 10^{-11} ergs cm^{-2} s^{-1}).

OBSERVATION OBJECT	OBSERVATION PERIOD	EXPOSURE (hr)	$F(>300\ \text{GeV})$ (f.u.) Fos/Cos	Extrapolated
1ES 0033+595	1995 Dec	1.85	2.04/0.25	<2.64
1ES 0145+138	1996 Oct–1996 Nov	7.85	.../...	<1.23
	1998 Nov–1998 Dec	2.29		<6.58
	1998 Dec–1999 Jan	1.98		<4.60
RGB J0214+517	1999 Dec–2000 Jan	6.01	5.93/0.07	<2.14
3C 66A...	1995 Oct–1995 Nov	8.00	0.14/...	<0.74
1ES 0229+200	1996 Nov–1996 Dec	7.85	0.96/0.31	<1.49
	1998 Nov–1998 Dec	2.30		<4.19
	1998 Dec–1999 Jan	1.78		<5.20
1H 0323+022	1996 Nov–1996 Dec	10.18	0.84/0.01	<2.39
	1997 Jan	0.91		<3.94
	1998 Dec–1999 Jan	3.18		<6.56
EXO 0706.1+5913.............................	1996 Dec	5.55	.../...	<1.15
	1997 Jan–1997 Mar	3.69		<2.13
	1998 Nov	1.83		<6.73
	1998 Dec–1999 Feb	1.90		<5.92
1ES 0806+524	1996 Feb–1996 Mar	5.57	1.36/...	<1.37
	2000 Jan–2000 Mar	4.16		<16.80
PKS 0829+046...................................	1995 Jan–1995 Apr	11.07	.../...	<1.47
1ES 0927+500	1996 Dec	5.08	.../...	<0.85
	1997 Jan–1997 Apr	5.04		<1.00
S4 0954+65..	1995 Feb–1995 Mar	3.70	.../...	<1.21
1ES 1028+511	1998 Dec–1999 Feb	4.43	0.43/...	<3.70
1ES 1118+424.....................................	1998 Feb–1998 Apr	7.30	.../...	<2.80
	1998 Dec–1999 Feb	3.60		<4.00
	2000 Jan–2000 May	6.97		<1.51
Mrk 40	2000 Jan–2000 Apr	10.16	.../...	<2.68
Mrk 180	1995 Jan–1995 Apr	5.55	8.50/0.03	<1.36
	1995 Dec–1996 May	20.46		<1.39
	1997 Jan	0.79		<4.00
1ES 1212+078	1999 Feb	1.13	.../...	<10.03
	2000 Jan–2000 May	3.70		<4.17
ON 325	1999 Feb	0.97	0.16/...	<11.37
	2000 Jan–2000 May	5.05		<2.79
1H 1219+301	1995 Jan–1995 May	2.77	0.67/0.16	<2.85
	1997 Feb–1997 Jun	11.27		<1.04
	1998 Jan–1998 Mar	1.38		<4.57
	1998 Dec–1999 Feb	2.94		<3.82
	2000 Jan–2000 Apr	3.69		<2.48
W Comae	1995 Feb–1995 Apr	14.33	.../...	<0.66
	1996 Jan–1996 May	15.73		<0.73
	1999 Jan–1999 Feb	4.43		<4.02
	2000 Jan–2000 Apr	4.72		<1.92
MS 1229.2+6430	1995 Feb–1995 Apr	1.39	.../...	<3.60
	1999 Feb	2.04		<5.75
	2000 Jan–2000 May	6.01		<2.21
1ES 1239+069	1999 Jan–1999 Feb	1.73	.../...	<7.94
	2000 Jan–2000 May	5.08		<2.56
1ES 1255+244	1997 Feb–1997 May	5.54	.../...	<1.48
	1998 Mar	0.46		<14.28
	1999 Feb	1.73		<6.55
	2000 Jan–2000 May	4.16		<2.13
OQ 530	1995 Mar–1995 May	7.39	.../...	<0.73
4U 1722+11	1995 Apr–1995 May	2.77	12.8/0.015	<1.56
I Zw 187	1995 Mar–1995 Apr	2.31	5.19/0.07	<1.08
	1996 Apr–1996 May	2.32		<1.98
1ES 1741+196	1996 May–1996 Jul	9.23	3.59/0.29	<0.70
	1998 May	0.46		<15.00
3C 371	1995 May–1995 Jun	13.04	.../...	<1.23
BL Lacertae......................................	1995 Jul	4.62	3.32/0.17	<1.37
	1995 Oct–1995 Nov	39.09		<0.50
	1998 May–1998 Jun	0.92		<22.12
1ES 2321+419	1995 Oct–1995 Nov	6.42	.../...	<1.33

NOTES.—Both the flux predictions and upper limits are given in absolute flux units (f.u., 10^{-11} ergs cm^{-2} s^{-1}). As was described in the text, the upper limits from Costamante & Ghisellini 2002 were calculated using two different approaches, that of Costamante (Cos) and that of Fossati (Fos).

REFERENCES

Aharonian, F. A., et al. 2000, A&A, 353, 847
Black, J. K., Brunton, A. N., Bannister, N. P., Deines-Jones, P., & Jahoda K. 2003, Nucl. Instrum. Methods Phys. Res. A, 513, 123
Blandford, R. D., & Levinson, A. 1995, ApJ, 441, 79
Bloom, S. D., & Marscher, A. P. 1996, ApJ, 461, 657
Böttcher, M., Muckherjee, R., & Reimer, A. 2002, ApJ, 581, 143
Bradbury, S. M., Burdett, A. M., D'Vali, M., Ogden, P. A., & Rose, H. J. 1999, in Proc. 26th Int. Cosmic Ray Conf. (Salt Lake City), 5, 263
Buckley, J. H. 1998, Science, 279, 676
Caccianiga, A., Maccacaro, T., Wolter, A., della Ceca, R., & Gioia, I. M. 1999, ApJ, 513, 51
Catanese, M., et al. 1997a, in AIP Conf. Proc. 410, Proc. Fourth Compton Symp., ed. C. D. Dermer, M. S. Strickman, & J. D. Kurfess (New York: AIP), 1376
———. 1997b, ApJ, 487, L143
———. 1998, ApJ, 501, 616
Cawley, M. F., & Weekes, T. C. 1995, Exp. Astron., 6, 7
Cawley, M. F., et al. 1990, Exp. Astron., 1, 173
Chadwick, P. M., Lyons, K., McComb, T. J. L., Orford, K. J., Osborne, J. L., Rayner, S. M., Shaw, S. E., & Turver, K. E. 1999, ApJ, 521, 547
Costamante, L., & Ghisellini, G. 2002, A&A, 384, 56
de la Calle Perez, I., et al. 2003, ApJ, 599, 909
Dermer, C. D., & Davis, S. P. 2000, in AIP Conf. Proc. 510, Proc. Fifth Compton Symp., ed. M. L. McConnell & J. M. Ryan (New York: AIP), 425
Dermer, C. D., & Schlickeiser, R. 1993, ApJ, 416, 458
———. 1994, ApJS, 90, 945
Dermer, C. D., Schlickeiser, R., & Mastichiadis, A. 1992, A&A, 256, L27
Djannati-Atai, A., et al. 2003, Proc. 28th Int. Cosmic Ray Conf. (Tsukuba), 5, 2575
D'Vali, M., et al. 1999, in Proc. 26th Int. Cosmic Ray Conf. (Salt Lake City), 3, 422
Fossati, G., Celotti, A., Ghisellini, G., & Maraschi, L. 1997, MNRAS, 289, 136
Fossati, G., Maraschi, L., Celotti, A., Comastri, A., & Ghisellini, G. 1998, MNRAS, 299, 433
Ghisellini, G. 1999, Astropart. Phys., 11, 11
Ghisellini, G., Celotti, A., Fossati, G., Maraschi, L., & Comastri, A. 1998, MNRAS, 301, 451
Ghisellini, G., & Madau, P. 1996, MNRAS, 280, 67
Grindlay, J. E., Craig, W. W., Geherls, N., Harrison, F. A., & Hong, J. 2003, Proc. SPIE, 4851, 331
Hartman, R. C., et al. 1999, ApJS, 123, 79
Helene, O. 1983, Nucl. Instrum. Methods Phys. Res., 212, 319
Hillas, A. M., et al. 1998, ApJ, 503, 744
Holder, J., et al. 2003, ApJ, 583, L9
Horan, D., et al. 2000, HEAD Meeting, 32, 05.03

Horan, D., et al. 2002, ApJ, 571, 753
———. 2004, in Proc. 2nd VERITAS Symp. on TeV Astrophysics of Extragalactic Sources (Amsterdam: Elsevier), in press
Jordan, M., et al. 2001, in Proc. 27th Int. Cosmic Ray Conf. (Hamburg), 7, 2691
Kerrick, A. D., et al. 1995, ApJ, 452, 588
Königl, A. 1981, ApJ, 243, 700
Krawczynski, H., et al. 2003, HEAD Meeting, 35, 49.01
Laurent-Muehleisen, S. A., Kollgaard, R. I., Feigelson, E. D., Brinkmann, W., & Siebert, J. 1999, ApJ, 525, 127
Mannheim, K. 1998, Science, 279, 684
Maraschi, L., Ghisellini, G., & Celotti, A. 1992, ApJ, 397, L5
Maraschi, L., et al. 1999, Astropart. Phys., 11, 189
Mücke, A., et al. 2003, Astropart. Phys., 18, 593
Neshpor, Y. I., Chalenko, N. N., Stepanian, A. A., Kalekin, O. R., Jogolev, N. A., Fomin, V. P., & Shitov, V. G. 2001, Astron. Rep., 45, 249
Neshpor, Y. I., et al. 1998, Astron. Lett., 24, 134
Nishiyama, T., et al. 1999, in Proc. 26th Int. Cosmic Ray Conf. (Salt Lake City), 3, 370
Padovani, P., & Giommi, P. 1995a, ApJ, 444, 567
———. 1995b, MNRAS, 277, 1477
Perlman, E. S., Padovani, P., Giommi, P., Sambruna, R., Jones, L. R., Tzioumis, A., & Reynolds, J. 1998, AJ, 115, 1253
Primack, J. R., Bullock, J. S., Somerville, R. S., & MacMinn, D. 1999, Astropart. Phys., 11, 93
Punch, M., et al. 1992, Nature, 358, 477
Quinn, J. 1998, Ph.D. thesis, National Univ. Ireland
Quinn, J., et al. 1996, ApJ, 456, L83
———. 1999, ApJ, 518, 693
Rebillot, P., et al. 2003, Proc. 28th Int. Cosmic Ray Conf. (Tsukuba), 5, 2599
Reynolds, P. T., et al. 1993, ApJ, 404, 206
Roberts, M. D., et al. 1998, A&A, 337, 25
———. 1999, A&A, 343, 691
Sikora, M., Begelman, M. C., & Rees, M. J. 1994, ApJ, 421, 153
Sikora, M., & Madejski, G. 2001, in AIP Conf. Proc. 558, High Energy Gamma-Ray Astronomy, ed. F. A. Aharonian & H. J. Völk (New York: AIP), 275
Stecker, F. W. 1999, Astropart. Phys., 11, 83
Tagliaferri, G., et al. 2000, A&A, 354, 431
Tluczykont, M., et al. 2003, Proc. 28th Int. Cosmic Ray Conf. (Tsukuba), 5, 2547
Urry, C. M., & Padovani, P. 1995, PASP, 107, 803
Vassiliev, V. V. 2000, Astropart. Phys., 12, 217
Veron-Cetty, M. P., & Veron, P. 1993, A&AS, 100, 521
Wagner, S. J., et al. 1995, A&A, 298, 688